The crystal structure of isotactic poly(methyl methacrylate): packing-mode of double stranded helices

Hiroshi Kusanagi*
Unitika Research Laboratories Inc., Kozakura, Uji, Kyoto 611, Japan

and Yozo Chatani and Hiroyuki Tadokoro
Department of Macromolecular Science, Faculty of Science, Osaka University, Toyonaka, Osaka 560, Japan
(Received 28 July 1993; revised 8 October 1993)

The X-ray structure analysis of isotactic poly(methyl methacrylate) was performed by adopting the 10/1 double-stranded helix model as the molecular model, and the crystal structure analysis, which has remained as an unsettled problem for a long time, has been brought to an end. The crystals are orthorhombic, with rather large cell dimensions, i.e. $a=41.96$, $b=24.34$, and c (fibre axis)$=10.50$ Å. There are eight 10/1 double-stranded helices of the right-handed and left-handed senses in the unit cell, which take up a slightly complicated hexagonal-like closest packing-mode, and where among the first six neighbour helices the two same-handed senses are located at $z=c/2$ and the four opposite-handed senses are located at $z=c/4$ and $3c/4$. The space group is Fddd-$D_{2h}{}^{24}$ for the disordered structure, which is composed of upward and downward helices related by a twofold rotation axis perpendicular to the helix axis. This complicated helical packing-mode originates from (i) the fact that iPMMA as synthesized is an apparently racemic polymer, and (ii) the fact that two molecular chains form a robust and rod-like 10/1 double-stranded helix.

(Keywords: isotactic poly(methyl methacrylate); crystal structure; X-ray analysis)

INTRODUCTION

After a long and somewhat roundabout quest the double-stranded helix was finally found in 1976 by the present authors[1] for the molecular structure of isotactic poly(methyl methacrylate) (iPMMA). The double-stranded helix structure, which was proposed then for the first time in synthetic polymers, is now accepted to be essentially correct from the results of many different kinds of studies, such as conformational energy calculations[2,3], Fourier transform infra-red (*FT*i.r.) spectroscopy[4], normal-mode calculations[5], and cross-polarization/magic angle spinning (CP/MAS) n.m.r. spectroscopy[6]. However, the crystal structure of iPMMA has not yet been analysed, and therefore, its complete structure determination has unfortunately remained an open problem[7,8].

The historical evolution of the proposed molecular models of iPMMA is summarized in *Figure 1*. A 5/2 helix (five monomeric units per two turns) model was first proposed (more than 35 years ago) by Stroupe and Hughes[9], while a 5/1 helix model was later reported by Liquori and coworkers[10–12]. In 1970, the present authors examined the possibilities of both models by using X-ray and infra-red spectroscopic data with isotactic-rich PMMA specimens, and they considered that the 5/1 helix was the most reasonable model at that time[13]. However, it was found that a narrow helix with a small radii, such as the 5/1 form, could not explain the strong X-ray reflection at the equator, nor the acceptable molecular arrangement in the orthorhombic lattice of $a=20.98$, $b=12.17$, and c (fibre axis)$=10.50$ Å. Therefore, we reexamined the molecular model by adopting some suggestions from energy calculations[14], and deduced at first a 10/1 double-stranded helix model[1], as shown in *Figure 1*. This double-stranded helix consists of two chains, denoted by continuous and broken lines in the figure, which are shifted by 10.50 Å along the helix axis from each other, and gives a fibre identity period of 10.50 Å, coinciding with the observed value, although each of the 10/1 helices has an identity period of 21.0 Å. The double-stranded helix was found to be more stable (by 4.4 kcal mol^{-1} of monomer unit) than two isolated 10/1 helices. The X-ray data can be considerably explained by a crystal structure consisting of two double-stranded helices, located in the centre and at the corner of the above orthorhombic lattice, resulting in an hexagonal-like closest packing of $a=12.2$ Å. However, the lowest discrepancy factor, R, used for evaluating the agreement between the observed and calculated X-ray intensities, was unfortunately 0.32, which is too large in comparison with the acceptable values of ~ 0.20 usually found in the crystal structure analysis of polymers[15]. After this, various other efforts were made by other researchers concerning the structure analysis. For example, another 10/1 double-stranded helix model, with different side-chain conformations, was proposed in 1982 by Challa and coworkers[16]: this model is essentially the same as ours. Most recently, the possibility of a non-helical model

* To whom correspondence should be addressed

0032-3861/94/10/2028–12

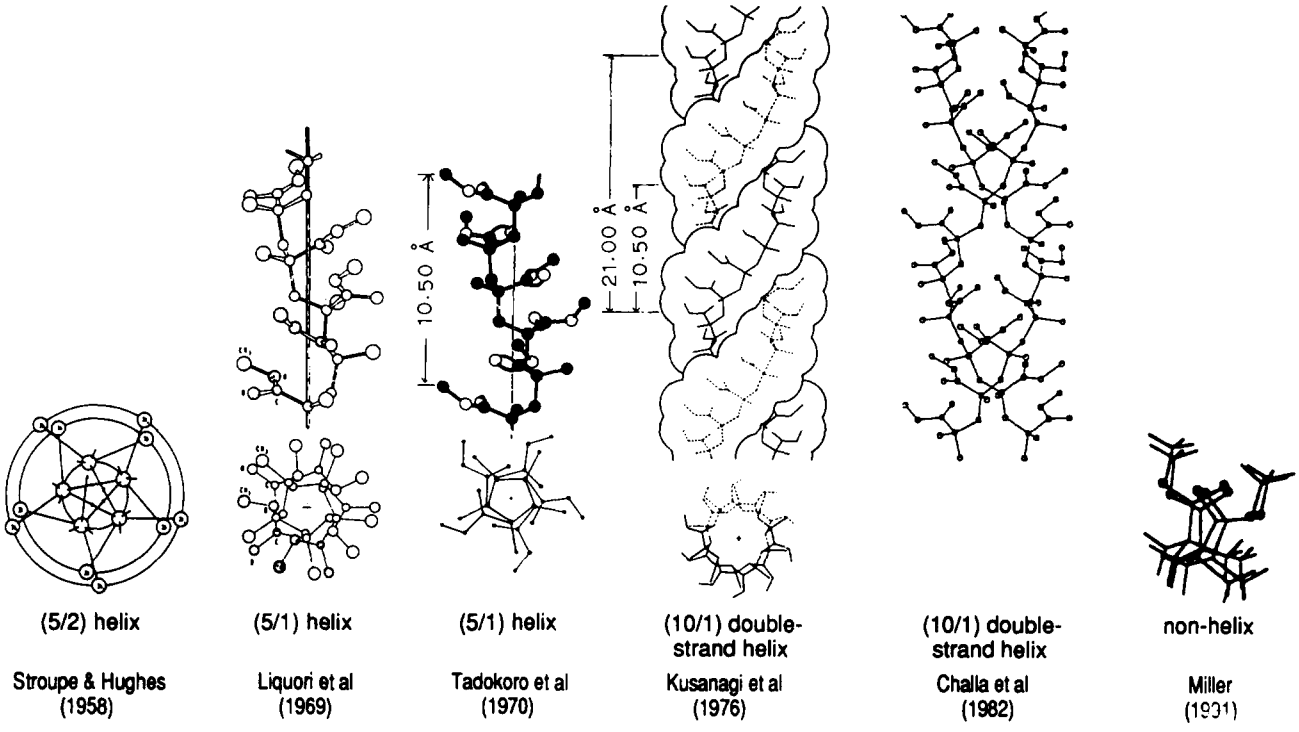

Figure 1 Evolution of proposed molecular models for iPMMA over the period from 1958 to 1991

was suggested[17], although this was largely to pose the question as to why the crystal structure cannot be solved by using the helix structure.

After all of this work, no one has succeeded in making a complete structure analysis up to this present time. Our double-stranded helix model could also not eventually overcome the difficulties in the various stages of molecular packing (crystal structure determination) in satisfactorily explaining the X-ray observed intensity data of iPMMA, and achieve a discrepancy factor R which was less than 0.20. One reason may be attributed to the accuracy of the 10/1 double-stranded helix model, i.e. the proposed double-stranded helix may be considerably different from the true double-stranded helix in the real crystal.

In this study, by the aid of computer calculations, we have been able to overcome these problems, and have searched for the key point parameters in the refinement of the 10/1 double-stranded helix model, and thus determined the crystal structure. Accordingly, we can report that the open problem of the crystal structure of iPMMA has now been brought to an end. In addition, we will consider in this report the background to the difficulties in the crystal structure determination of iPMMA as a typical, difficult example of the structure determination of synthetic polymers.

EXPERIMENTAL

Samples of iPMMA were kindly supplied by Dr Y. Kotake of the Research Laboratory, Mitsubishi Rayon Company. The tactic index I (triad) measured by n.m.r. spectroscopy is approximately 100%. Uniaxially oriented specimens for the X-ray measurements were prepared by casting from toluene solution, stretching to approximately five to ten times the original lengths, and subsequent heat-treatment at 90°C for 6 h under vacuum.

The X-ray diffraction measurements were made with nickel-filtered Cu Kα radiation by using cylindrical cameras with radii of 5 and 10 cm. Weissenberg photographs were taken by setting the oriented specimen with the oriented direction perpendicular to the camera axis. *Figure 2* shows X-ray photographs of iPMMA obtained in this way. The diffraction intensity was measured by the multiple-film method, with 49 independent reflections being observed. The reflection intensities were then estimated by visual comparison with a standard intensity scale, and were corrected for the single-crystal rotation Lorentz-polarization factor.

DETERMINATION OF STRUCTURE

Our historical summary of the crystal structure determination of iPMMA is shown in *Figure 3*. The early stages of the structure determination (up to 1977) is described in a review[18] by Tadokoro, one of the present authors. At the beginning of this present study, there are three important points to bear in mind concerning the analysis:

1. The setting up of molecular models is carried out by using energy calculations so as to take into account all of the possible models.
2. For the decision concerning the space group, we use the correspondence between the symmetry property of the crystal lattice and the three-dimensional features of the molecular model: (i) there are four kinds of the 10/1 double-stranded helices, namely right-up (RU), right-down (RD), left-up (LU), and left-down (LD); (ii) each helix has a twofold rotation axis coinciding with the helix axis and; (iii) each helix has a rod-like shape which seems to be suitable for an hexagonal closest-packing arrangement in the crystal (see *Figure 1*). This is a new approach for determining the space group in a structure analysis in which the characteristic features of molecular models are available.
3. For the final stage of the analysis, we designed a suitable computer software program to enable us

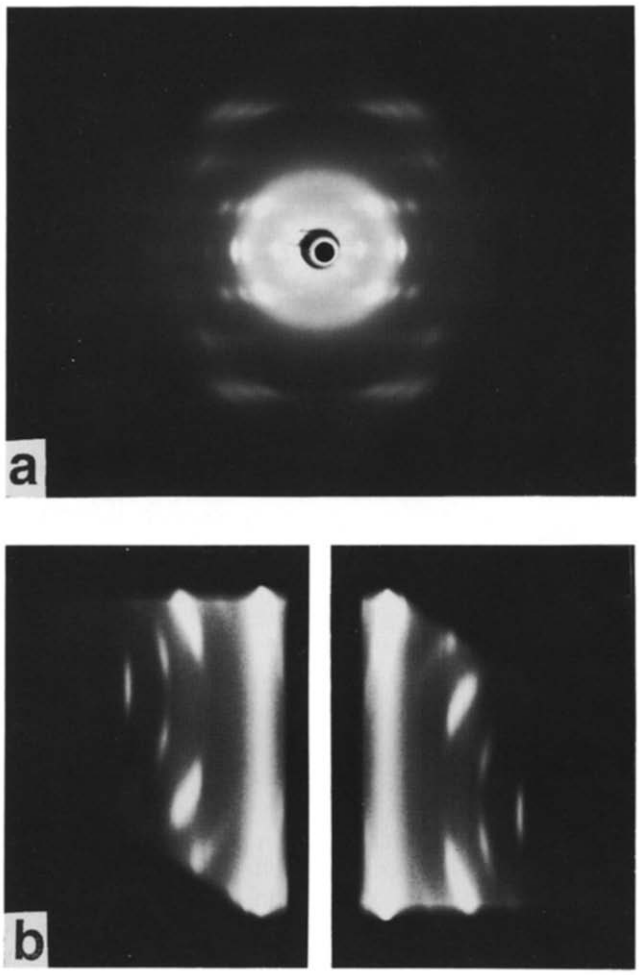

Figure 2 X-ray photographs of iPMMA: (a) fibre diagram and; (b) Weissenberg diagram taken with the rotation axis perpendicular to the fibre axis

to search for the most effective conformational parameters for a reduction in the *R*-factor, as it was not possible to use the least-squares refinement procedure owing to the small ratio of the intensity data to the parameter numbers.

Setting up of a molecular model

The atoms and the internal rotation angles are numbered as follows:

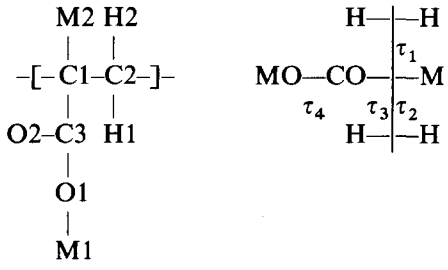

The internal coordinates are the same as those used in ref. 1. The molecular conformation can be deduced if the four kinds of internal rotation angles are determined. First, the internal rotation angles τ_1 and τ_2 of the skeletal chain were calculated to be -179 and $-148°$, respectively, by using the helical parameter equation[19], assuming a 10/1 helix with a period of 21.0 Å. Hereinafter, we will consider only right-handed helices. Secondly, the two internal rotation angles of the side chain, i.e. τ_3 and τ_4, were examined by conformational energy calculations. The use of energy calculations with regard to intramolecular interactions is a useful technique for setting up molecular models, but it does also have a limit to its applicability in polymer crystal structure analysis[20]. The calculation was carried out by using the same procedure as described in ref. 13, with the molecular parameters and potential constants used being the same as those given in ref. 14. There are two energy contour maps, depending on whether the ester group points upwards, with the α-CH_3 group pointing outward, or the reverse applies. The allowable range for τ_3 and τ_4 is very small, because of the bulky α-CH_3 and ester side-groups. From the two energy minima found in each map when plotted against τ_3 and τ_4, four stable 10/1 single helix models were obtained. The internal rotation angles and potential energies are listed in *Table 1*. Model I,

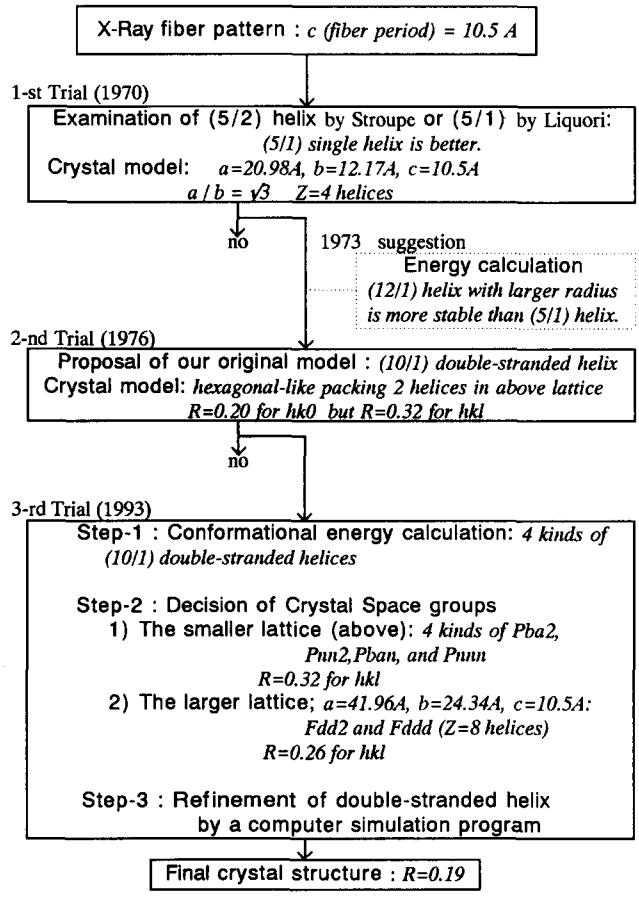

Figure 3 Historical summary of the crystal structure determination process of iPMMA

Table 1 Energetically stable 10/1 single helix conformations of iPMMA

Model	τ_1 (deg)	τ_2 (deg)	τ_3 (deg)	τ_4 (deg)	E^a	E^b
α-CH_3 pointing outwards						
Model I	−179	−148	−30	180	4.2	−5.4
Model II	−179	−148	165	175	13.6	105.8
α-CH_3 pointing inwards						
Model III	−179	−148	−40	185	18.8	−3.9
Model IV	−179	−148	140	185	19.1	−3.8

[a] Intramolecular potential energy of a single chain (kcal per mole of monomer unit)
[b] Intermolecular potential energy between two intertwined chains (kcal per mole of monomer unit)

proposed in 1976[1], has the lowest potential energy, while models II, III, and IV all have fairly large energies. Moreover, the 10/1 double-stranded helices were composed of two single helices, shifted 10.5 Å along the axis of the helix with respect to each other, and the intermolecular interaction energies between these were calculated for all of the models. The results indicated that the double-stranded helix is more stable, by 5.4, 3.9, and 3.8 kcal per mole of monomer unit, for models I, III, and IV, respectively, than two isolated 10/1 helices, while model II was unsuccessful in achieving intertwining of the two molecular chains, because of the very large repulsive potential energy of 105.8 kcal mol^{-1}. From these energy calculations, it seems that model I is the most probable one. *Figure 4* shows four types of 10/1 double-stranded helix models, viewed along the helix axis: it can be clearly seen that they have very different conformations to each other.

Unit cell and space group

The equatorial reflections of the fibre photograph were indexed with a hexagonal unit cell of $a=12.2$ Å, while all of the reflections could be indexed using an orthorhombic unit cell, with $a=20.98$, $b=12.17$, and c (fibre axis) $=10.50$ Å. By assuming that two double-stranded helices, with ten chemical units in the fibre identity period, are contained in the unit cell, the density is calculated as 1.26 g cm^{-3}, which is acceptable when compared with the observed density, i.e. 1.21 g cm^{-3}. The apparent systematic absences of the reflections, $(h+k)$ odd for $hk0$, suggest that the two double helices pass through the centre and the corner of the unit cell. In addition, the axial ratio, a/b ($\approx\sqrt{3}$) corresponds to an hexagonal packing ($a=12.2$ Å) of the double helices, as mentioned above. However, a determination of the space group is rather difficult to achieve from the reflection data alone, because of the small number, the overlapping nature, and the broadness of the reflections. Therefore, we tried to determine the possible space group by consideration of the relationship between the space group symmetry[21] and the geometrical properties of 10/1 double-stranded helices.

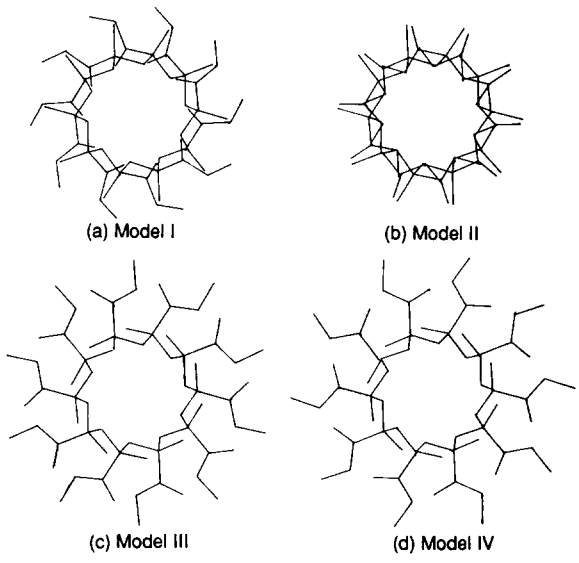

Figure 4 Energetically stable 10/1 single-helix models of iPMMA viewed along the helix axis: (a) Model I; (b) Model II; (c) Model III and; (d) Model IV

The possible orthorhombic space groups are reduced to four types by applying the following considerations:

1. The total number of possible space groups belonging to the orthorhombic lattice (i.e. 59) reduces to 50, since non-optically active iPMMA, which has both right-handed and left-handed helices, should have an achiral lattice.
2. Among these, 17 space groups could contain two strands in the lattice by satisfying the hexagonal-closest-packing mode.
3. In addition, among these 17 space groups 13 groups which require a crystallographic, statistically-disordered structure composed of right- and left-handed helices are rejected as the result of an established theory: the disordered structures of both 'upward' and 'downward' helices are known cases[22,23].
4. Finally, only four space groups, both of the ordered structure, namely Pba2 and Pnn2, and also the disordered structure with respect to the 'up–down' statistics, i.e. Pban and Pnnn, remain as possible candidates.

Crystal structure

The calculation of the structure factors was performed, assuming the space groups of Pba2, Pnn2, Pban, and Pnnn for three of the molecular models (with the exception of model II), by trial-and-error procedures, in which both the position of the double-stranded helices along the twofold axis of the lattice, and the setting angle about this axis, were varied. The discrepancy factor R $(=\sum|\sqrt{I_0}-\sqrt{I_c}|/\sum\sqrt{I_0})$, where $I_c=\sum mF^2$, I_0 and I_c are, respectively, the observed and calculated X-ray reflection intensities, m is the multiplicity of the reflection, and F is the structure factor of the reflection, is 0.20 or less for the equatorial reflections for any combination of the helix models and space groups. However, the agreement between the observed and calculated intensities for the layer lines is unsatisfactory, especially for the first layer line, e.g. strong intensity reflection of 211, and non-observed reflections of 201 and 301. This situation suggests that the packing-mode of the double-stranded helices is wrong and therefore urges us to consider four or more double-stranded helices. We examined again the 57 space groups belonging to the orthorhombic system, and found that Pba2 and Pnn2 are within the subgroup of Fdd2, while Pban and Pnnn are within the subgroup of Fddd. For these new space groups the unit cell has twice the a- and b-dimensions of the above orthorhombic cell, and contains eight double-stranded helices.

Therefore, the crystal structures with the space groups Fdd2-C_{2v}[19] and Fddd-D_{2h}[24], with $a=41.96$, $b=24.34$, and $c=10.50$ Å, were adopted for the structure-factor calculation. As a result of this, these Fdd2 and Fddd crystal models reduced the R factor to 0.28 (or close to this value) for all of the reflections. However, any crystal model gives the problem that some of the inter-helix atomic distances of 3.24 Å and less (for CH_3–CH_3) are too short, and are therefore not acceptable. These short distances are attributed to the structure itself, i.e. in comparison with the distance of 12.2 Å among the adjacent helices, the helix radii of the outer ester CH_3 groups are large, with values of 4.7, 5.1, and 5.3 Å, for models I, III, and IV, respectively. There is no way to

avoid this problem except for an improvement in the helix models, leading towards smaller radii.

As the next step, we designed a computer software program which could simultaneously calculate the structure factors and the inter-helix atomic distances (van der Waals contact distances) by using the internal coordinates as the input parameters, so as to carry out the trial-and-error calculation in a very short period of time. The results showed that among the internal coordinates the torsion angles, as well as the bond angles, have an influence on the van der Waals contact distances, and, in particular, the helix radii of the side chain atoms depend strongly on two bond angles, namely θ_1 (CH_2–C–CH_2) and θ_2 (C–CH_2–C), and two torsion angles i.e. τ_1 and τ_2, of the skeletal chain, while the torsion angles τ_3 and τ_4 are restricted to their initial values (or close to them), due to the very high potential barriers. Consequently, the conformation of the skeletal chain contains the key parameters for the improvement of the molecular models, and in addition the entire structure is extensively varied by them, so that a reduction in the *R*-factor must be expected.

We tried to refine all of the 10/1 double-stranded helices, including model II, which now could intertwine with a double-stranded helix, after the molecular model improvement process. For these models, the structure factors were calculated for the Fddd and Fdd2 lattices, in which the molecular parameters (bond length, bond angle, and torsion angle), the height of the helices along the twofold axis, and the setting angle about the twofold axis, were examined. Among these, the crystal structure of molecular model III reduced the *R*-factor to 0.18 and 0.21, for the Fddd and Fdd2 space groups, respectively, and also had reasonable van der Waals contact distances, i.e. CH_3–$CH_3 \geqslant 3.88$ Å, CH_3–$O \geqslant 2.92$ Å, etc. Similar values for the closest CH_3–CH_3 distances for intermolecular interactions have been reported, e.g. 3.71 and 3.88 Å for polyisobutylene[24], and 3.81 Å for poly(dimethyl ketene)[25].

If the space group Fdd2 is assumed, the crystal consists of either upward or downward helices, with respect to right- and left-handed senses. On the other hand, if the space group Fddd is assumed, upward and downward helices coexist at the same lattice points with the same probability in the crystal lattice, the so-called crystallographic, statistically-disordered structure[22,23]. By comparing values of the *R*-factor, the iPMMA crystal should have the Fddd space group and take a statistically-disordered structure consisting of upward and downward helices in a ratio of 1:1. For the sake of simplicity, however, the crystal structure represented by the Fdd2 space group is shown in *Figure 5*. From this representation of the molecular packing in the crystal lattice, the reliability of the final crystal structure is easily seen. *Figure 6* shows a representative crystal section which is obtained by cutting the crystal lattice at $z = 5c/8$, and is drawn in terms of the van der Waals molecular model. Accordingly, it is understandable that the molecular packing is appropriate as a whole, and interactions between the intertwined two chains are strong (close-good van der Waals contacts), while interactions between the double-stranded helices are somewhat weak (loose-poor van der Waals contacts). The final molecular structure is shown in *Figure 7*, with the final atomic coordinates for the 10/1 helix given in *Table 2*, and the observed and calculated structure factors listed in *Table 3*. In the structure-factor calculation, the hydrogen atoms were included, and an isotropic temperature factor of 12.0 Å^2 was assumed for all of the atoms.

RESULTS AND DISCUSSION

Molecular structure

The final 10/1 double-stranded helix has a symmetrical and elegant shape when viewed along the fibre axis, compared with the initial models shown in *Figure 4*. An approximate mirror symmetry, which passes through the fibre axis, appears in the final structure. This mirror symmetry comes from the D_2 molecular symmetry of the skeletal chain, i.e. a twofold rotation axis, perpendicular to the helix axis, passes through each skeletal C1 atom and the helix axis. This situation is quantitatively due to the same values of the torsion angles $\tau_1 = -162°$ ($-179°$) and $\tau_2 = -163°$ ($-148°$), and also the bond angles

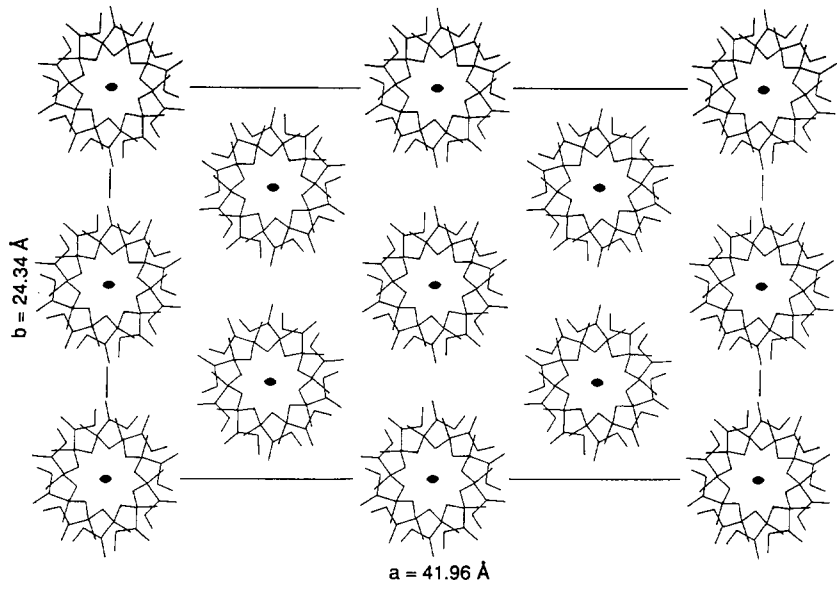

Figure 5 Crystal structure of iPMMA, drawn according to the Fdd2 space group for simplicity: only upward double-stranded helices are shown

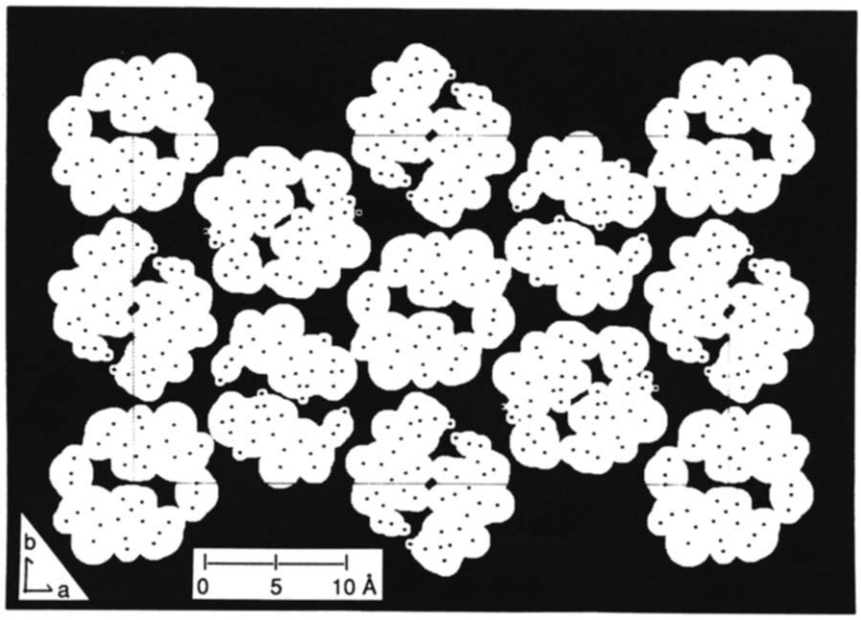

Figure 6 Sectional plane of the crystal structure of iPMMA at $z = 5c/8$, presented in terms of the van der Waals molecular model

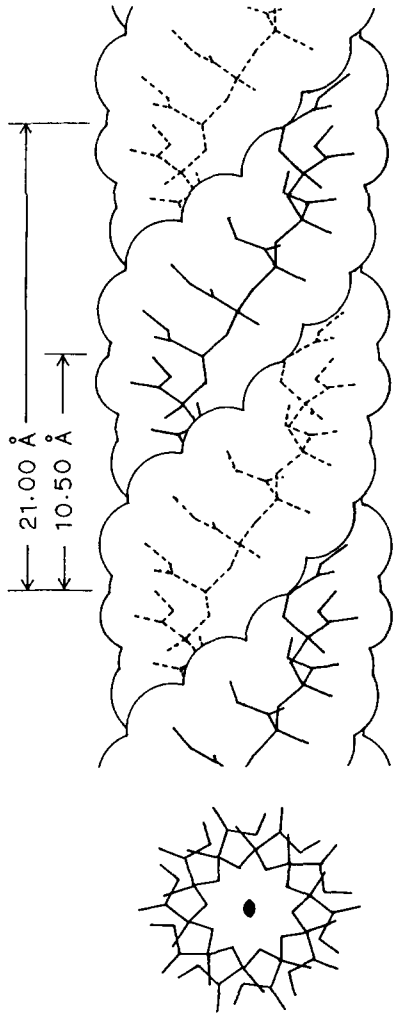

Figure 7 The final molecular structure of iPMMA containing the 10/1 double-stranded helix

$\theta_1 = 124°$ (124°) and $\theta_2 = 104°$ (109.5°), being different considerably from the initial values given in parentheses. Large deviations of θ_1 ($= 124°$) and θ_2 ($= 104°$) from the tetrahedral angle of 109.5° are acceptable, because they

Table 2 Fractional and cylindrical atomic coordinates of iPMMA[a]

Atom	x	y	z	r (Å)	y (deg)	z (Å)
C1	0.0653	−0.0098	0.1150	2.751	0.0	0.000
C2	0.0440	0.0181	0.0160	1.898	−18.4	−1.039
C3	0.0832	−0.0547	0.0441	3.737	15.9	−0.745
O1	0.0617	−0.0912	0.0002	3.441	35.6	−1.205
M1	0.0756	−0.1295	−0.0855	4.471	39.8	−2.105
O2	0.1126	−0.0587	0.0269	4.937	11.8	−0.925
M2	0.0912	0.0273	0.1734	3.883	−14.8	0.614
H1	0.021	−0.044	0.164	1.37	46.0	0.51
H2	0.034	0.007	0.268	1.44	−12.0	1.61
H11	0.086	−0.108	−0.168	4.44	31.0	−2.97
H12	0.057	−0.158	−0.119	4.54	53.0	−2.45
H13	0.095	−0.152	−0.037	5.43	38.0	−1.59
H21	0.107	0.042	0.098	4.61	−18.0	−0.18
H22	0.105	0.004	0.243	4.41	−6.0	1.34
H23	0.080	0.062	0.221	3.68	−29.0	1.12

[a] Equivalent atoms in the monomer unit are located at $(-x, -y, z)$. The coordinates of other monomer units are defined by the 10/1 helical symmetry

are close to the values of 124.6° and 103.5° which have been obtained in the crystal structure analysis of methyl methacrylate oligomers[26].

Each polymer chain is practically a 10/1 single helix with an identity period of 21.0 Å. As shown in *Figure 7*, the double-stranded helix consists of two single helices, with the same helix sense and direction, which are shifted 10.50 Å along the helix axis with respect to each other. Consequently, the double-stranded helix has a half-identity-period of 10.50 Å (the observed fibre identity period) corresponding to the single helix period of 21.0 Å. This double-stranded helix thus constituted has a twofold rotation axis and its symmetry coincides with the twofold rotation axis in a crystal lattice with a Fddd space group. These correspondences between the molecular and crystal symmetries are quite reasonable.

It would seem to be very interesting to clarify the reasons why iPMMA does form the double-stranded helix, although there is no strong interactions between the two helices, such as, for example, hydrogen bonding in DNA[27,28] and poly(ethylene imine) (PEI)[29].

Table 3 Observed and calculated intensities of iPMMA, with I_c calculated for the Fddd space group[a]

Indices	ξ_c[b]	ξ_0[b]	$\sqrt{I_0}$[c]	$\sqrt{I_c}$[d]
4 0 0	0.147	0.147	358	339
2 2 0	0.146			
0 4 0	0.253	0.254	393	446
6 2 0	0.254			
8 0 0	0.294	0.294	283	282
4 4 0	0.293			
10 2 0	0.389	0.388	129	132
8 4 0	0.388			
2 6 0	0.387			
12 0 0	0.441	0.440	60	88
6 6 0	0.439			
12 4 0	0.509	0.508	81	72
0 8 0	0.507			
14 2 0	0.530	0.529	103	125
10 6 0	0.529			
4 8 0	0.528			
16 0 0	0.588	0.587	86	100
8 8 0	0.586			
2 10 0	0.638	0.640	64	98
14 6 0	0.640			
16 4 0	0.640			
6 10 0	0.671	0.672	59	61
12 8 0	0.672			
18 2 0	0.673			
10 10 0	0.732	–	(8)	17
20 0 0	0.735			
0 12 0	0.760	0.770	68	58
18 6 0	0.763			
4 12 0	0.774			
16 8 0	0.776			
20 4 0	0.777			
8 12 0	0.815	0.816	81	58
14 10 0	0.816			
22 2 0	0.818			
1 1 1	0.073	0.073	42	23
3 1 1	0.127	0.127	70	51
1 3 1	0.194	0.194	379	342
5 1 1	0.194			
3 3 1	0.220	0.220	42	62
5 3 1	0.264	0.265	143	145
7 1 1	0.265			
1 5 1	0.319	0.320	116	114
7 3 1	0.320			
3 5 1	0.335	0.335	126	127
9 1 1	0.337			
5 5 1	0.366	0.379	60	24
9 3 1	0.381			
7 5 1	0.408	0.408	52	45
11 1 1	0.409			
1 7 1	0.445	0.457	90	60
11 3 1	0.447			
3 7 1	0.457			
9 5 1	0.458			
5 7 1	0.480	0.481	71	57
13 1 1	0.482			
7 7 1	0.513	0.513	64	48
11 5 1	0.513			
13 3 1	0.514			
9 7 1	0.553	0.566	85	56
15 1 1	0.555			
1 9 1	0.571			
13 5 1	0.573			

Table 3 *continued*

Indices	ξ_c[b]	ξ_0[b]	$\sqrt{I_0}$[c]	$\sqrt{I_c}$[d]
3 9 1	0.581	0.588	98	85
15 3 1	0.583			
5 9 1	0.599			
11 7 1	0.600			
7 9 1	0.625	–	(29)	100
17 1 1	0.628			
15 5 1	0.636			
13 7 1	0.652	0.655	93	113
17 3 1	0.653			
9 9 1	0.659			
1 11 1	0.698	0.700	120	123
11 9 1	0.699			
17 5 1	0.700			
19 1 1	0.701			
3 11 1	0.705			
15 7 1	0.707			
5 11 1	0.721			
19 3 1	0.724			
7 11 1	0.743	0.760	99	105
13 9 1	0.744			
17 7 1	0.766			
19 5 1	0.767			
9 11 1	0.771			
21 1 1	0.774			
2 0 2	0.073	–	(4)	0
0 2 2	0.127	–	(4)	3
2 2 2	0.146	–	(4)	4
4 2 2	0.194	–	(4)	9
6 0 2	0.220	–	(4)	2
6 2 2	0.254	0.257	46	36
2 4 2	0.264			
4 4 2	0.293	0.293	51	49
8 2 2	0.320	0.330	97	120
6 4 2	0.336			
10 0 2	0.367	0.373	146	128
0 6 2	0.380			
2 6 2	0.387	0.388	154	187
8 4 2	0.388			
10 2 2	0.389			
4 6 2	0.407	–	(29)	55
6 6 2	0.439	0.442	73	70
10 4 2	0.446			
12 2 2	0.459			
8 6 2	0.480	–	(37)	62
12 4 2	0.509	0.509	95	52
2 8 2	0.512			
14 0 2	0.514			
4 8 2	0.528	0.529	105	74
10 6 2	0.529			
14 2 2	0.530			
6 8 2	0.553	–	(21)	11
14 4 2	0.573	0.580	91	84
12 6 2	0.582			
8 8 2	0.586			
16 2 2	0.601	–	(29)	36
10 8 2	0.626	0.635	91	88
0 10 2	0.633			
2 10 2	0.638			
14 6 2	0.640			
16 4 2	0.640			

continued

Table 3 *continued*

Indices	ξ_c[b]	ξ_0[b]	$\sqrt{I_0}$[c]	$\sqrt{I_c}$[d]
4 10 2	0.650			
18 0 2	0.661			
6 10 2	0.671	0.670	81	86
12 8 2	0.672			
18 2 2	0.673			
1 1 3	0.073	–	(4)	2
3 1 3	0.127	–	(4)	14
1 3 3	0.194			
5 1 3	0.194	0.195	131	94
3 3 3	0.220			
5 3 3	0.264	0.265	120	84
7 1 3	0.265			
1 5 3	0.319			
7 3 3	0.320	0.320	211	198
3 5 3	0.335			
9 1 3	0.337			
5 5 3	0.366	0.365	100	104
9 3 3	0.381	0.380	108	147
7 5 3	0.408	0.410	53	65
11 1 3	0.409			
1 7 3	0.445			
11 3 3	0.447	–	(29)	84
3 7 3	0.457			
9 5 3	0.458			
5 7 3	0.480	–	(29)	50
13 1 3	0.482			
7 7 3	0.513			
11 5 3	0.513	–	(29)	24
13 3 3	0.514			
9 7 3	0.553			
15 1 3	0.555			
1 9 3	0.571	0.578	96	67
13 5 3	0.573			
3 9 3	0.581			
15 3 3	0.583			
5 9 3	0.599			
11 7 3	0.600			
7 9 3	0.625	0.620	103	120
17 1 3	0.628			
15 5 3	0.636			
13 7 3	0.652			
17 3 3	0.653	0.655	96	73
9 9 3	0.659			

[a] Discrepancy factor R ($=\sum(\sqrt{I_0}-\sqrt{I_c})/\sum\sqrt{I_0}$) is 0.18 for all I_0 values, when including the observed threshold, and 0.15 for all I_0 values when excluding the observed threshold

[b] $\xi=\sqrt{(\sin\theta)^2-(l\lambda/c)^2}$

[c] Values of $\sqrt{I_0}$ in parentheses indicate the observed threshold

[d] $\sqrt{I_c}$ is equivalent to $\sqrt{(\sum mF^2)}$

Energy calculations give a large stabilization energy of 5.4 kcal per mole of monomer unit, owing to just the van der Waals interaction between the two intertwined chains. For the double-stranded helix some sliced sectional planes normal to the helix axis are shown in *Figure 8*, presented in terms of the van der Waals molecular model. A perfect van der Waals fitting between the two intertwined chains is easily seen and the origin of the stabilizing energy, i.e. the driving force for intertwining, can be readily understood.

It is possible to construct a double-stranded helix model with some stabilizing energy which is composed of two anti-parallel single helices, as in DNA. However, its occurrence in the real crystal was denied by the X-ray data. The real double-stranded helix has a direction of either upwards or downwards, since it consists of two single helices with the same direction, and therefore has a dipole moment which is parallel to the helix axis. The dipole moment of the parallel double-stranded helices is negated by pairs of anti-parallel double-stranded helices within the Fddd space group (the up–down disorder structure). The dipole moment of a double-stranded helix is actually expected to be small, since the dipole moments of the polar ester groups are almost normal to the helix axis (see *Figure 6*). Therefore, the electrostatic energy difference between the parallel and the anti-parallel arrangements of the double-stranded helices may also be small. If the crystals with the up–down disorder corresponding to the Fddd space group are poled by a strong electric field, they might transform into the ordered structure, which corresponds to the Fdd2 space group. Of course, polymorphism has not yet been found in iPMMA, but it is conceivable that crystal modifications may be identified in the future.

In addition, the double-stranded helix of iPMMA clarifies the structure of the stereocomplex of isotactic and syndiotactic PMMA[30].

Packing-modes of double-stranded helices

The crystal structure of iPMMA has been clearly settled by the X-ray structure analysis: the *R*-factor is 0.18 for all of the observed intensities including the observed threshold, and 0.15 when the latter is excluded. The crystals have a rather large unit cell, which belongs to the Fddd space group, and also a rather complicated molecular arrangement, composed of eight double-stranded helices. In this section, we want to determine the basis for this structure from the packing geometry of the double-stranded helices. *Figure 9* shows schematically the packing-mode of the double-stranded helices in the final crystal structure (with the Fdd2 space group), when compared with examples of other, smaller unit cells. During the process, it was found that the final crystal structure could be represented by using a monoclinic unit cell which contains four double-strained helices, with the following cell parameters: $a=13.25$, $b=41.96$, $c=10.50$ Å, and $\beta=113.33°$. This medium-sized unit cell with the lower space group ($P2_1/a$) is shown in *Figure 9c*. The space groups Fddd and Fdd2 correspond to the monoclinic C2/c and Cc space groups, except that the helix does not possess a twofold rotation axis in these cases. Moreover, the lattice corresponding to the space group $P2_1/a$ displays another packing-mode for the double-stranded helices. Here, we consider, for simplicity, the ordered structure with the space group Fdd2 instead of Fddd. For iPMMA, there are four kinds of 10/1 double-stranded helices: right-up (RU) and left-down (LD) from the apparent D-isomer, and right-down (RD) and left-up (LU) from the apparent L-isomer[31]. The Fdd2 lattice has eight 10/1 double-stranded helices, with right-handed and left-handed senses, in the unit cell, assuming a slightly complicated hexagonal-like closest packing-mode, where among the six first neighbour helices the two same-handed senses are located at $z=c/2$, while the four opposite-handed senses are located at $z=c/4$ and $3c/4$. The $P2_1/a$ lattice contains all of the four kinds of helices and yet can still take an ordered structure. This packing-mode is the most reasonable, but is impossible in the real crystal because of a more

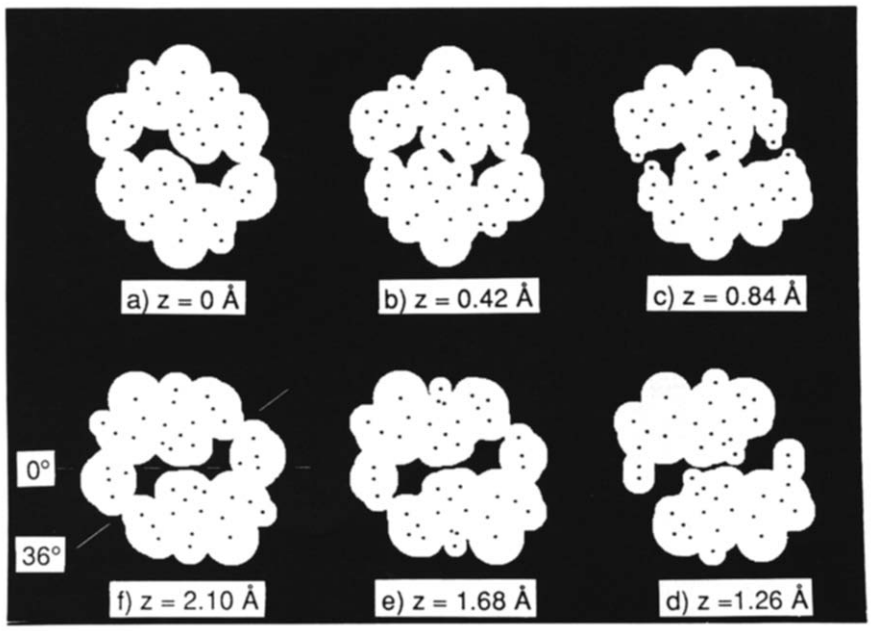

Figure 8 Sliced sectional planes of double-stranded helices, normal to the helix axis, of iPMMA. (a) and (f) are separated by 2.1 Å (= 10.5 Å/5 monomers) along the helix axis, and are rotated by 36° (= 360° × (1/10)) to each other. A perfect van der Waals fitting between the two intertwined chains can be easily seen

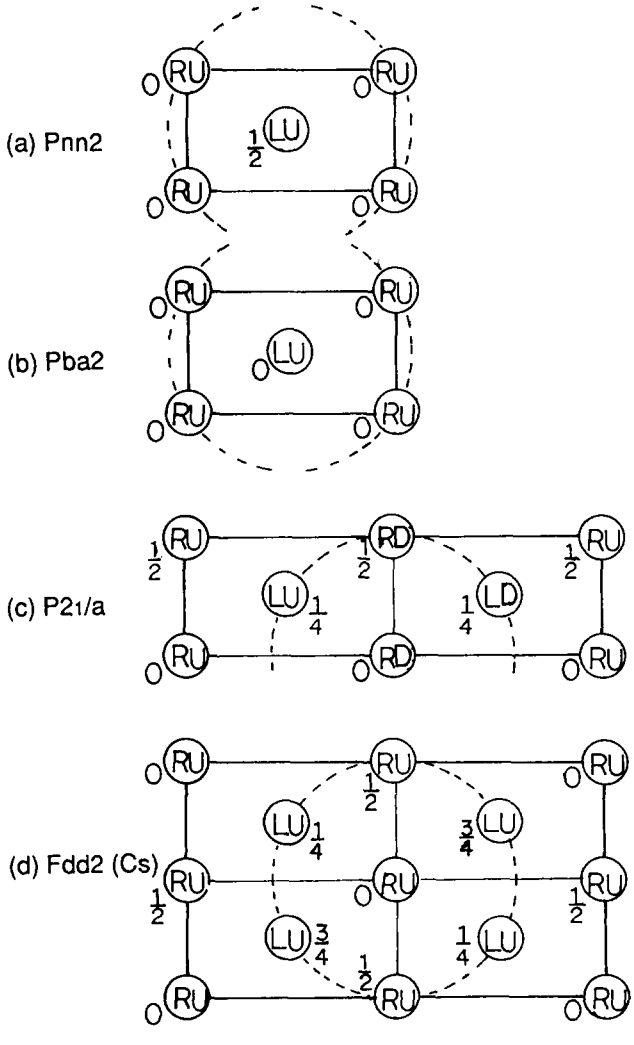

Figure 9 Schematic representations of the packing-modes of double-stranded helices with respect to various space groups: (a) Pnn2; (b) Pba2; (c) $P2_1/a$ and; (d) Fdd2 (Cs)

Table 4 Dependency of *R*-factor on unit cell size and space group

Unit cell size	Small	Small	Medium	Large
Number of helices in unit cell	2	2	4	8
Space group[a]	Pnn2	Pba2	$P2_1/a$	Fdd2(Cc)
R-factor	0.41	0.36	0.35	0.21
Space group[b]	Pnnn	Pban	–	Fddd(C2/c)
R-factor	0.45	0.40	–	0.18

[a] Ordered structure
[b] Disordered structure with the helix direction either upwards or downwards

complicated packing-mode: i.e. it is difficult for the robust 10/1 double-stranded helices to change the handed senses of the helix and/or to exchange their locations in the lattice with respect to each other when they crsytallize. On the other hand, the Pba2 lattice has the most simple packing-mode, i.e. where six surrounding double-stranded helices are located at the same height. In addition, six strands shift by $c/2$ in the Pnn2 lattice. For these crystal lattice models, the structure factors were calculated and compared with the observed structure factors. The *R*-factors for all of the reflections are listed in *Table 4*. Accordingly, the Fddd (Fdd2) lattice is selected as the best in terms of the X-ray data, i.e. the *R*-factor and the comparison between the calculated and observed intensities on the first layer lines. This situation is understandable from the packing geometry, namely the visualization of the packing-mode of the strands. *Figure 10* shows sliced sectional planes of the crystal lattice at $z=0$ to $4c/5$, with an interval of $\Delta z=c/5$, presented in terms of the van der Waals molecular model. From these figures, it can be intuitively understood that the Fdd2 lattice has a better packing-mode than the Pba2 lattice (of the same-handed sense) between the two adjacent double-stranded helices along the *b*-axis. This is because these two helices, which are located at the

same height, come into close contact at $z=c/5$ and $4c/5$, due to the twofold rotation (C_2) symmetry of the double-stranded helix. The space group of the PEI anhydrate is the first reported case in which 5/1 double-stranded helices take the Fddd space group[29], while the second case is probably in the crystal structure of iPMMA, as reported here.

Finally, the complicated helical packing-mode of iPMMA seems to originate from (i) the fact that iPMMA as synthesized is an apparently racemic polymer, and (ii) the fact that two molecular chains form a robust and rod-like double-stranded helix.

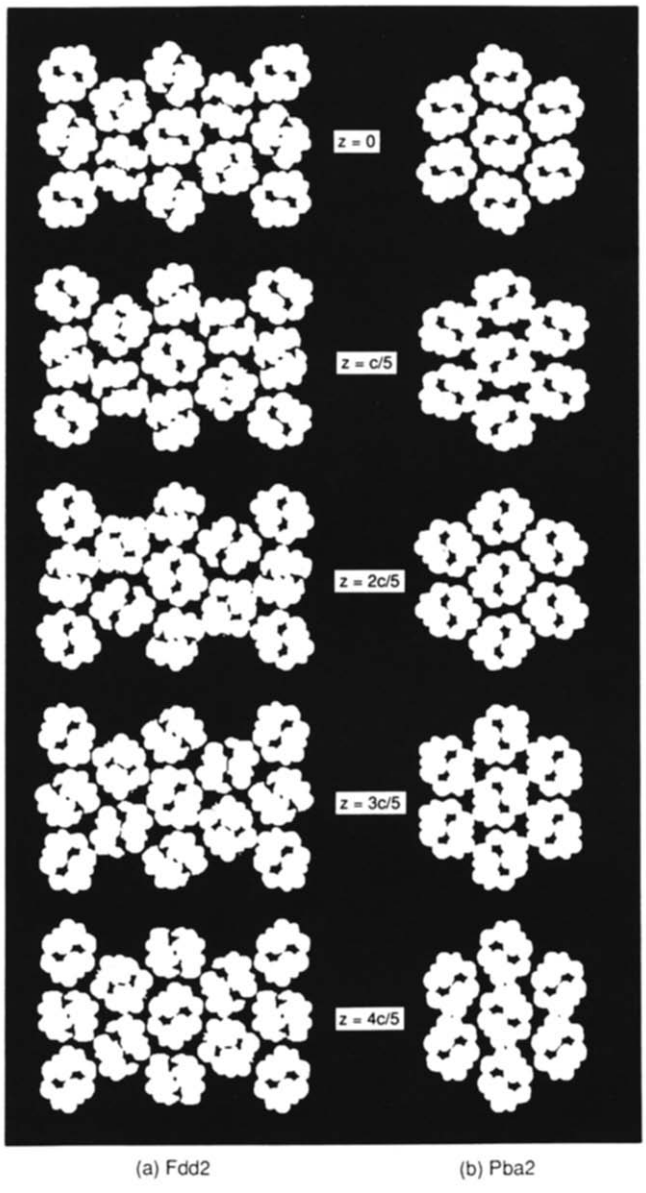

Figure 10 The van der Waals contacts among the first neighbour double-stranded helices from the viewpoint of lattice sections from $z=0$ to $4c/5$, where the origin of the z-axis is shifted $5c/8$ from that shown in *Figure 6*: (a) Fdd2 (large lattice) and; (b) Pba2 (small lattice)

Relation of molecular symmetry and crystal structure

As mentioned above, one reason that the double-stranded helices of iPMMA pack in a hexagonal-like closest packing might be attributed to their rod-like shape. However, since these helices have no trigonal or hexagonal symmetry properties, such as e.g. poly(oxymethylene) (POM)[32,33], this hexagonal-like closest packing of the iPMMA crystals is quite remarkable. We will consider this aspect now in more detail. In the hexagonal-closest packing the coordination number of the first neighbouring helices is six. Therefore, three molecular sectional planes, related by a sixfold rotation symmetry coinciding with the helix axis, should help to clarify the situation. *Figure 11* shows three such planes of iPMMA (10/1), POM (9/5), and isotactic polypropylene (iPP) (3/1) helices, possessing C_2, C_9^s, and C_3^s molecular symmetry, respectively. Even if the helices do not strictly belong to the trigonal or hexagonal space groups, they will most often take the hexagonal-like closest packing arrangement, if they have three molecular sections with similar outlines to each other. POM is, of course, strictly trigonal, while the double-stranded helices of iPMMA is the case possessing the similar outlines. Among these three polymers, the 3/1 helix of iPP, having three mutually different molecular sections, takes a packing-mode which is quite different from the hexagonal-closest packing[22]. Consequently, it is emphasized that we should pay attention to the practical molecular symmetry (i.e. the molecular outline) when considering the relationship between molecular symmetry and crystal structure.

Difficulty of crystal structure analysis of iPMMA

The crystal structure analysis of synthetic polymers, which can only give the X-ray fibre diagrams (i.e. two-dimensional data), is made essentially, even at the present time, by a trial-and-error method. In addition, it is not possible to proceed directly from the above two-dimensional data to the final structure, when

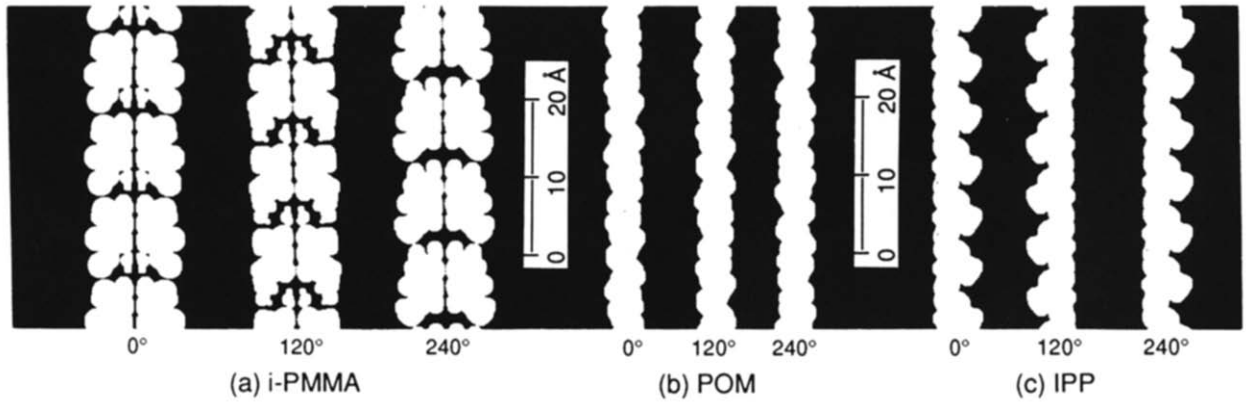

Figure 11 Three molecular sectional planes, related by a sixfold rotation symmetry, passing through the helix axis of: (a) iPMMA; (b) POM and; (c) iPP

Table 5 Comparison between the internal coordinates of the initial model III and the final 10/1 helix conformation of iPMMA

Bond lengths Bond	Initial	Final	Bond	Initial	Final
C1–C2	1.53	1.53	C3–O2	1.21	1.25
C2′–C1	1.53	1.53	O1–M1	1.46	1.42
C1–C3	1.54	1.52	C1–M2	1.54	1.54
C3–O1	1.36	1.35	C–H	1.10	1.10
Bond angles **Angle**	**Initial**	**Final**	**Angle**	**Initial**	**Final**
C2′–C1′–C2	109.5	103.7	C1′–C2–C1	124.0	124.0
C2′–C1–C3	109.5	106.0	C1–C3–O1	116.0	108.0
C2′–C1–M2	109.5	115.0	C1–C3–O2	120.0	128.0
C2–C1–C3	109.5	115.5	O1–C3–O2	124.0	124.0
C2–C1–M2	109.5	111.5	C3–O1–M1	114.0	112.0
C3–C1–M2	109.5	105.5	Other angles	109.5	
Torsion angles **Angle**	**Initial**	**Final**			
C2′–C1–C2–C1″	−178.8	−161.8			
C1′–C2′–C1–C2	−147.5	−162.6			
C1′–C2′–C1–C3	92.5	75.4			
C1′–C2′–C1–M2	−27.5	−40.7			
C2′–C1–C3–C1	80.0	63.0			
C1–C3–O1–M1	185.0	190.0			
M2–C1–C3–O1	−160.0	−174.7			

[a] The atoms are numbered as follows:

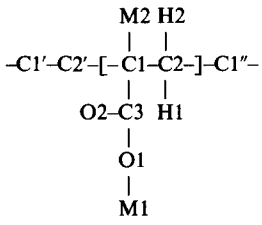

compared to the direct method, in which three-dimensional X-ray data is obtained for single crystals[34]. The final 10/1 double-stranded helix conformation that we obtained here is very different from the starting model deduced from energy calculations (see *Figures 4* and *7*, and *Table 5*). Moreover, the least-squares refinement procedure is also impossible to use for improvement of the molecular models, because of the small ratio of the intensity data (49) to the number of variable parameters (>70).

Finally, it is concluded that because the true structure of iPMMA was of an unexpected new type (the double-stranded helix), with the assumed model being extremely different from the correct structure, the analysis was therefore very difficult, took a long time to complete, and involved much detailed thought.

REFERENCES

1 Kusanagi, H., Tadokoro, H. and Chatani, Y. *Macromolecules* 1976, **9**, 531
2 Sundararajan, P. R. *Macromolecules* 1986, **19**, 415
3 Vacatello, M. and Flory, P. J. *Macromolecules* 1986, **19**, 405
4 Brinkhuis, R. H. G. and Schoutten, A. J. *Macromolecules* 1991, **24**, 1496
5 Dybal, J. and Krimm, S. *Macromolecules* 1990, **23**, 1301
6 Spevacek, J., Schneider, B. and Straka, J. *Macromolecules* 1990, **23**, 3042
7 Coiro, V. M., Liquori, A. M., De Santis, P. and Mazzarella, L. *J. Polym. Sci. Polym. Lett. Edn* 1978, **16**, 33
8 Lovell, R. and Windle, A. H. *Macromolecules* 1981, **14**, 211
9 Stroupe, J. D. and Hughes, R. E. *J. Am. Chem. Soc.* 1958, **80**, 2341
10 D'Alagni, M., De Santis, P., Liquori, A. M. and Savino, M. *J. Polym. Sci. (B)* 1964, **2**, 925
11 Liquori, A. M., Anzuno, Q., Coiro, V. M., D'Alagni, M., De Santis, P. and Savino, M. *Nature (London)* 1965, **206**, 358
12 Coiro, V. M., De Santis, P., Liquori, A. M. and Mazzarella, L. *J. Polym. Sci. (C)* 1969, **16**, 4591
13 Tadokoro, H., Chatani, Y., Kusanagi, H. and Yokoyama, M. *Macromolecules* 1970, **3**, 441
14 Tadokoro, H., Tai, K., Yokoyama, M. and Kobayashi, M. *J. Polym. Sci., Polym. Phys. Edn* 1973, **11**, 825
15 Tadokoro, H. 'Structure of Crystalline Polymers', Wiley, New York, 1979, p. 159
16 Bosscher, F., ten Brinke, G., Eshuis, A. and Challa, G. *Macromolecules* 1982, **15**, 1364
17 Miller, K. J. *Macromolecules* 1991, **24**, 6877
18 Tadokoro, H. *Polymer* 1984, **25**, 147
19 Miyazawa, T. *J. Polym. Sci.* 1961, **55**, 215
20 Kusanagi, H., Tadokoro, H., Chatani, Y. and Suehiro, K. *Macromolecules* 1977, **10**, 405
21 Henry, N. F. and Lonsdale, K. 'International Tables for X-Ray Crystallography', Vol. I, 2nd Edn, Kynoch Press, Birmingham, 1965, p. 73
22 Natta, G. and Corradini, P. *Nuovo. Cimento., Suppl.* 1960, **15**, 40
23 Natta, G., Corradini, P. and Bassi, I. W. *Nuovo Cimento., Suppl.* 1960, **15**, 68
24 Tanaka, T., Chatani, Y. and Tadokoro, H. *J. Polym. Sci., Polym. Phys. Edn* 1974, **12**, 515
25 Bassi, I. W., Ganis, P. and Temussi, P. A. *J. Polym. Sci. (C)* 1967, **16**, 2867

26 Ute, K., Nishimura, T., Matsuura, Y. and Hatada, K. *Polymer J.* 1989, **21**, 231
27 Watson, J. D. and Crick, H. C. *Nature (London)* 1953, **171**, 737
28 Langrige, R., Wilson, H. R., Hooper, C. W. and Wilkins, M. H. F. *J. Mol. Biol.* 1960, **2**, 19
29 Chatani, Y., Kobatake, T., Tadokoro, H. and Tanaka, R. *Macromolecules* 1982, **15**, 170
30 Schomaker, E. and Challa, G. *Macromolecules* 1989, **22**, 3337
31 Tadokoro, H. 'Structure of Crystalline Polymers', Wiley, New York, 1979, p. 376
32 Uchida, T. and Tadokoro, H. *J. Polym. Sci. (A-2)* 1967, **5**, 63
33 Takahashi, Y. and Tadokoro, H. *J. Polym. Sci., Polym. Phys. Edn* 1979, **17**, 123
34 Tadokoro, H. 'Structure of Crystalline Polymers', Wiley, New York, 1979, p. 6